UNIVERSITY OF LJUBLJANA
FMF
Faculty of Mathematics and Physics

Department of Physics

Seminar I - 1st year, 2nd cycle

Generating Entangled Photon Pairs Using Nonlinear Crystal With Type-II SPDC

Author: Gaja Šalamun

Advisor: dr. Peter Jeglič
Co-advisor: dr. Izidor Benedičič

Ljubljana, April 2025

Abstract

Entanglement is a quantum phenomenon involving two or more particles, where particles are described by a single wavefunction that cannot be separated into sub-particle states. In this seminar, I will present one possible platform for generation of entangled photon pairs. The basis for this method is a spontaneous parametric downconversion process in a nonlinear crystal inside the Sagnac interferometer. First, the setup of the experiment and its elements are described and results obtained in the Laboratory for Quantum Entanglement at IJS are presented. Similar sources can be used to build a quantum network that promises more secure communication than classical channels. The main challenge is overcoming large distances since quantum systems decohere very fast. At the end, I also present the current record for entanglement distribution over long distances using optical fibers.

1 Introduction

Quantum physics has become an integral part of understanding basic building blocks of matter and has fundamentally changed our understanding of nature, leading to some of the largest technological advancements. Quantum systems have been used to perform some of the most precise measurements that exceed the limits of classical systems. Quantum physics can also be used to construct more secure communication channels or networks. The field of quantum computing also promises exponentially faster solutions to certain computational problems compared to a classical computer [1]. They are routinely implementing the ability to control individual quantum systems, which was once only a theoretical dream. They rely on three important properties of quantum systems. Quantum superposition allows a system to occupy multiple states at the same time. Quantum entanglement generates nonclassical correlations between the states of distinct subsystems. Quantum measurement collapses the superposition into one single state. Quantum technologies are currently interesting both technologically and scientifically [1–4].

Interaction of quantum systems with outside environment perturbs the system, causing decoherence, and is often the limiting factor [5]. As a result, scaling quantum systems to larger networks, such as connecting two cities or countries, remains a significant difficulty. Photonics is one of the most technologically advanced fields to date, allowing us to precisely control and manipulate photons with minimal losses or perturbations. Thus, photons can be used as the basis of a quantum system [2, 4].

In this seminar, I will present a widely used method for generating entangled photons enabling applications in quantum communication. We will focus on photons that are entangled in their polarization state and link two stationary nodes in a quantum system, laying the groundwork for quantum communication. Photon entanglement can be achieved via light-matter interaction in a nonlinear crystal. The crystal can be placed inside a Sagnac interferometer, creating a robust source of entangled photons that are immune to small mechanical perturbations of the optical setup. The use of (entangled) photons for quantum technologies often relies on precise characterization of quantum state. This is done by performing a set of measurements and reconstructing the quantum state using quantum state tomography [6–9].

2 Quantum Network

The term quantum network refers to several separate nodes (laboratories) where each node has its own quantum system that stores quantum information in some number of quantum bits (qubits), which are processed locally using quantum gates. Nodes are interconnected by communication channels through which quantum signals are sent. Together, they form a larger and more complex quantum system [3].

The most practical way to exchange and connect quantum states between individual nodes is to send light through optical fibers. The state can be encoded by their polarization, frequency, or phase which is later connected to the classical bits 0 and 1. They travel with the speed of light and are therefore ideal for transporting information over large distances while exploiting their ability to maintain a state of superposition and low losses in fibers. Fibers must be isolated from other telecommunication signals, as they could interfere with our quantum signal and add background noise that worsens the quality of the state. It offers us secure data transmission through protocols such as quantum key distribution and quantum state teleportation, as the principles of quantum mechanics prevent access to its information or its cloning without tampering with the quantum state. We also cannot amplify quantum signals, as this would constitute a quantum measurement that would change the state of the photon. Therefore, because of the absorption of light in the glass (the core of the optical fiber), we are limited to distances of a few hundred kilometers. Longer distances for the distribution of quantum states can be achieved using entanglement swapping [2, 4].

Another way to achieve longer distances, as well as to bridge over natural barriers (e. g. seas), is by using satellites. In free space, the transmission losses are smaller and enable a direct link to thousands of kilometers. The downside of this approach is that they use visible and near-infrared wavelengths that are strongly affected by atmospheric phenomena [10].

3 Entanglement

Entanglement is a phenomenon that can only be described using quantum mechanics and therefore has no classical counterpart. If two (or more) particles are entangled, they will be more strongly correlated than classical physics allows. Particles will be described by a single wavefunction, which cannot be separated into sub-particle states. It plays a key role in various implementations of quantum computation, quantum communication, quantum key distribution, cryptography, teleportation, etc. For the aforementioned applications the fundamental unit is a qubit, which can be realized using any general two-level quantum system. Photons are especially useful because they propagate through space.

We can write any single qubit state as: $|\psi\rangle = \sum_i c_i |\phi_i\rangle$, where $\sum_i |c_i^2| = 1$ and where $\{|\phi_i\rangle\}$ forms an orthonormal basis in the Hilbert space. A two-qubit system is described by the tensor product of those two otherwise independent systems: $|\psi_{AB}\rangle = |\psi\rangle_A \otimes |\psi\rangle_B$.

Using photons as qubits, one can write states in their polarization. Since light is an electromagnetic wave that has oscillating orthogonal electric and magnetic field components, we can regard the polarization as the direction of the electric field of the light wave. The state of a linearly polarized photon can be written as a superposition of two orthogonal polarizations: $|\psi\rangle = \alpha |H\rangle + \beta\ e^{i\phi} |V\rangle$, where $|H\rangle$ represents the horizontal polarization, $|V\rangle$ the vertical polarization, and ϕ represents the phase between the two-photon pairs. Polarization can be written in different bases, such as diagonal $|D\rangle$ and anti-diagonal $|A\rangle$ or right circular light $|R\rangle$ and left circular light $|L\rangle$, which are all superpositions of $|H\rangle$ and $|V\rangle$. The product of two states with well-defined polarizations can be written as a product state:

$$\begin{aligned} |\psi\rangle = |\psi\rangle_1 \otimes |\psi\rangle_2 &= \left(\alpha_1 |H\rangle_1 + \beta_1 e^{i\phi_1} |V\rangle_1\right) \otimes \left(\alpha_2 |H\rangle_2 + \beta_2 e^{i\phi_2} |V\rangle_2\right) = \\ &= c_1\ |H\rangle_1 |H\rangle_2 + c_2\ |H\rangle_1 |V\rangle_2 + c_3\ |V\rangle_1 |H\rangle_2 + c_4\ |V\rangle_1 |V\rangle_2\ , \end{aligned} \tag{1}$$

where c_1 is a constant. We get a superposition of four possible two-particle states, each with its own probability amplitude. In such states, we can see the state of each subsystem separately. We call them separable states. However, not all possible states are product states, and we can have a statistical mixture of states. For this, we need the density matrix formalism [6].

Representing a quantum state using density matrices is particularly useful in situations where the wavefunction is insufficient to describe the system. This may occur when the state is mixed or after measurements have been performed on the system. Generally, we can write the density operator as:

$$\hat{\rho} = \sum_i p_i |\psi_i\rangle \langle\psi_i|\ , \tag{2}$$

where $p_i \geq 0$ and $\sum_i p_i = 1$. They can be separated into two groups: pure and mixed states. If we have all the information about the system, then the state is a pure state. The density matrix is written as the outer product of the wavefunction: $\hat{\rho} = |\psi\rangle\langle\psi|$. A mixed state corresponds to a probabilistic mixture of pure states. Unlike pure states, a mixed state cannot be decomposed into wavefunctions and is written as Eq. 2, where $\mathrm{Tr}(\rho^2) < 1$.

For a mixed state, the density matrix is written as:

$$\rho\ =\ \begin{array}{c} \\ |HH\rangle \\ |HV\rangle \\ |VH\rangle \\ |VV\rangle \end{array} \!\!\begin{array}{c} \begin{array}{cccc} \langle HH| & \langle HV| & \langle VH| & \langle VV| \end{array} \\ \begin{pmatrix} A_1 & B_1 e^{i\phi_1} & B_2 e^{i\phi_2} & B_3 e^{i\phi_2} \\ B_1 e^{i\phi_1} & A_2 & B_4 e^{i\phi_4} & B_5 e^{i\phi_5} \\ B_2 e^{i\phi_2} & B_4 e^{i\phi_4} & A_3 & B_6 e^{i\phi_6} \\ B_3 e^{i\phi_3} & B_5 e^{i\phi_5} & B_6 e^{i\phi_6} & A_4 \end{pmatrix} \end{array} \tag{3}$$

where A_i, B_i are real and ϕ_i is the phase between the two-photon pairs.

A state is entangled if it is not separable, meaning that we cannot write it as a product state like Eq. 1. Particles cannot be described separately, so the results of measurements on an individual particle are correlated. This means that if one particle is measured, accurate predictions can be made about the state of the other entangled particle. The most common examples are so-called *Bell states*:

$$|\psi^{\pm}\rangle = \frac{1}{\sqrt{2}} \left(|H\rangle_1 |V\rangle_2 \pm |V\rangle_1 |H\rangle_2\right) \tag{4}$$

$$|\phi^{\pm}\rangle = \frac{1}{\sqrt{2}} \left(|H\rangle_1 |H\rangle_2 \pm |V\rangle_1 |V\rangle_2\right) \tag{5}$$

which are maximally entangled, meaning that states have a maximum correlation with each other. They form a basis for all two-qubit states.

Another example of maximally entangled states is the so-called *GHZ states*:

$$|GHZ\rangle = \frac{1}{\sqrt{2}} \left(|H\rangle^{\otimes n} \pm |V\rangle^{\otimes n}\right)\ , \tag{6}$$

where we can generalize them for n qubits, where $n \geq 3$ [6, 7].

3.1 Characteristic of Entangled States

To check the quality of the entangled state, one needs to calculate its characteristics. Properties that describe it are directly derived from the density matrices.

Fidelity is a characteristic that tells us how close the real state is to the target state. For pure states, it is given by a scalar product between the two states ρ_1 and ρ_2: $F = |\langle\rho_1|\rho_2\rangle|^2$. It tells us the state overlap. More general definition is:

$$F(\rho_1, \rho_2) = \left(Tr\left(\sqrt{\sqrt{\rho_1}\rho_2\sqrt{\rho_1}}\right)\right)^2 , \tag{7}$$

where $0 \leq F(\rho_1, \rho_2) \leq 1$ and the higher the fidelity, the higher the overlap with the target state [6].

Purity gives us information on how much a state is mixed and is defined as:

$$\gamma = Tr\{\rho^2\} . \tag{8}$$

If the quantum state is pure, then the purity will be $\gamma = 1$ and if it is mixed, the purity will be strictly less than 1, with the lower limit being 0 [2, 7].

Tangle is a measure of the entanglement of a two-qubit state that can be computed from the expression of concurrence C:

$$T = (C(\rho))^2 = (max(0, \lambda_1 - \lambda_2 - \lambda_3 - \lambda_4))^2 , \tag{9}$$

where λ_i denotes the i^{th} eigenvalue of a matrix $R = \sqrt{\sqrt{\rho}\tilde{\rho}\sqrt{\rho}}$, where λ_1 is the highest eigenvalue and $\tilde{\rho} = (\sigma_y \otimes \sigma_y)\rho^*(\sigma_y \otimes \sigma_y)$, where ρ^* is the complex conjugate of ρ and σ_y is the Pauli-y matrix. Tangle ranges from 0 for a separable state to 1 for a maximally entangled state [6].

4 Spontaneous Parametric Downconversion

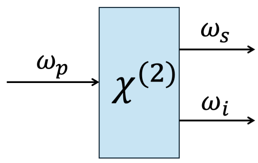

Figure 1: SPDC process in a nonlinear crystal when phase mismatch is zero. Pump photon with frequency ω_p splits into two photons with energies ω_s and ω_i.

One of the possible ways to generate entangled photons is spontaneous parametric downconversion (SPDC). This is a second-order nonlinear optical effect. When a pump photon with frequency ω_p enters the material, it spontaneously splits into two photons (usually called *signal* s and *idler* i) each with a portion of the initial energy and frequencies ω_i and ω_s (Fig. 1). It is a strictly quantum effect and cannot be explained in terms of classical nonlinear optics and needs quantization of the electromagnetic field.

In SPDC, the *parametric* part indicates that the energy is conserved and that the susceptibility that describes the process is real and not imaginary. The *spontaneous* part indicates that it is a very inefficient process (of the order $\sim 10^{-4}$) [6]. When generating entanglement, inefficiency is actually a benefit, since increasing it also increases the probability to create multiple photon pairs at once. That would lead to a decrease in the entanglement generated. The *downconversion* part indicates that a photon with high energy is converted to low-energy photons.

SPDC is the time-reversed process of sum-frequency generation (SFG or SHG). It uses an interacting Hamiltonian with two terms, each describing one of the possible processes that compete [11].

It is characterized to be of three types. In type-II, the downconverted photons have orthogonal polarization and one has the same polarization as the incoming photon. In type-I the downconverted photons have the same polarization that is orthogonal to the polarization of the incoming photon. In type-0 downconverted photons have the same polarization as the incoming photon [11].

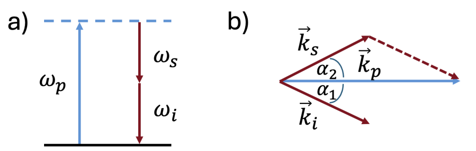

Figure 2: Phase matching conditions. a) Representation of energy conservation of SPDC. b) Representation of momentum conservation of SPDC.

The photons generated in SPDC follow the energy conservation rule (Fig. 2 a) so that: $\omega_p = \omega_s + \omega_i$. They also need to fulfill the momentum conservation rule (Fig. 2 b):

$$\Delta\vec{k} = \vec{k_p} - \vec{k_s} - \vec{k_i} . \tag{10}$$

Eq. 10 is called the phase matching condition and $\Delta\vec{k}$ is called phase mismatch. In order to achieve efficient SPDC the phase mismatch has to be zero.

This is related to the fact that the pump beam must remain in phase with the signal and idler beams to allow the signal power to constructively interfere throughout the crystal. To achieve efficient SPDC, the phase mismatch must approach zero, which can be achieved in various ways [6, 7, 11].

4.1 Nonlinear Crystals

In order to satisfy phase matching condition, one needs to have $k_p = k_s + k_i$, where using $k_j = \frac{n_j \omega_j}{c}$, for $j = p,\ s,\ i,$ we can rewrite it as:

$$\frac{n_p \omega_p}{c} = \frac{n_s \omega_s}{c} + \frac{n_i \omega_i}{c}\,, \tag{11}$$

which is impossible to satisfy in most materials because for normal dispersion we have $n_i(\omega_i) < n_s(\omega_s) < n_p(\omega_p)$ for $\omega_i < \omega_s < \omega_p$. That is where we need birefringent crystals since they possess two (uniaxial) or three (biaxial) different refractive indices (n_e and n_o for extraordinary and ordinary indices) along different symmetry axes for a given wavelength [11].

Birefringence is an optical effect that can occur in nonlinear optical materials. It describes the dependence of the refractive index of the material on the polarization of the light and the propagation direction of the light. This type of phase matching is called *birefringent phase matching*, where a crystal needs to be cut in a very specific way, aiming to achieve $\Delta k = 0$ by having the correct angle between the wave vector of the photon and the crystal axis. Due to birefringence of the crystal, the distribution of the signal and idler photons will be cone-like.

For type-II phase matching, the cones have the same origin, but they do not overlap. If the crystal is cut correctly, the two cones will intersect along two lines. When a photon is detected along one of these lines and if signal and idler have the same wavelength, we will not know from which cones the photon came. We will not know its polarization, but we will know that the other photon of the pair will have come along the other intersection. The general state of the two photons is described by Eq. 4. This photon generation scheme is illustrated in Fig. 3 [6, 7, 11].

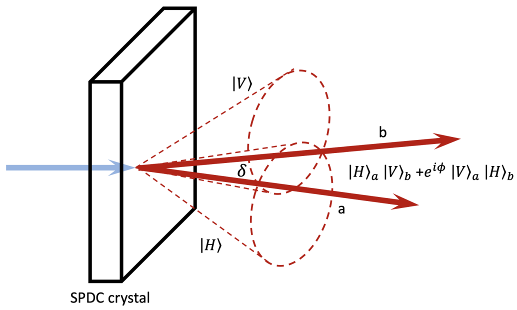

Figure 3: Type II SPDC single emitter source of entangled photons. The signal and idler photons are ecah emitted along a cone-like surface and intersect along two lines (a and b). Photons collected along these two intersections can be maximally entangled [7].

One thing that we need to take into account when dealing with SPDC is that the input beam and the generated beams do not travel in the same direction. This is called a walk-off. Temporal walk-off, also known as longitudinal walk-off, comes from the fact that the crystal has two indices along which downconverted photons follow. They will travel with different velocities, meaning that one photon will come out of the crystal before the other. This difference is given by $\Delta t = \left| L_c \left(\frac{1}{n_e} - \frac{1}{n_o} \right) \right|$, where L_c is the length of the crystal. The spatial walk-off or transverse walk-off is a consequence of the birefringence of the material. The energy propagation is not necessarily in the same direction as the wave vector of the dowconverted photons for the ordinary wave o but not for the extraordinary wave e. Therefore, we end up with an angle δ between the two waves at the output of the crystal: $\delta = -\frac{1}{n_e}\frac{dn_e}{d\theta}$, where θ is the angle of pump photons with the optical axis. This limits the length of the crystal that can be used because at some point the walk-off becomes larger than the beams [11].

4.2 Quasi-phase Matching

In the previous section, we saw that for SPDC to occur, the phase mismatch Δk must approach zero. Because of the dispersion in the material and longitudinal walk-off, it is hard to satisfy the Eq. 10. That means that one needs to compensate for the phase drift. One possible solution is to modify the material to change the effective refractive indices for the photons. The first two methods that one can use are temperature and angle tuning, but both have limitations with the length of the crystal that can be used. An alternate approach is quasi-phase matching (QPM), where the nonlinear medium is periodically reversed and consequently the sign of the nonlinear susceptibility is periodically reversed throughout the medium [12]. Because of this, the phase matching condition changes, and we get an additional term in our equation:

$$\vec{k_p} = \vec{k_s} + \vec{k_i} + \vec{K_G} \tag{12}$$

where $\vec{K_G}$ is the QPM grating vector $\left(K_G = \frac{2\pi}{\Lambda}\right)$ and Λ is the polling period. Eq 12 is called quasi-phase matching condition and depends on the period Λ, where the typical values for Λ are $10 - 100$ μm. It gives a new parameter that can be chosen freely in order to satisfy the phase matching condition. Therefore, angle tuning is not needed, which leads to two distinct advantages. With the right period Λ, one can create a collinear downconversion that is phase matched. This makes it much easier to collect all of the downconverted photons produced. The second advantage is that one can now choose one of the crystal's crystallographic axes for the beams to travel along. This will eliminate spatial wall-off problems and allows much larger crystals to be used, again leading to an increased signal [7, 8, 12]. QPM also allows us to achieve type-0 phase matching, where the polarizations of all photons are the same [8].

4.3 Periodic Poling

In the previous section, it was assumed that we could periodically reverse the sign of the nonlinear coefficient, without explaining how this can actually be done. One possible way is to cut a nonlinear crystal into thin slices and then reassemble it by rotating every second slice by 180°. Theoretically, this would work, but the problem with this method is that in order to satisfy Eq. 12 one would need Λ to be of the order $1 - 100$ μm, which makes this method impractical [13].

Another way in which one can fabricate nonlinear crystal for QPM is periodic poling [12]. This method works for ferroelectric materials. The idea behind it, shown in Fig. 4, is to apply electrodes on a crystal, once every period. When voltage is applied to these electrodes, an electric field is created in the material which inverts the orientation of the domains, therefore inverting the sign of $\chi^{(2)}$. The materials most commonly used for periodic poling are lithium niobate ($LiNbPO_3$ or LN) family, lithium tantalate ($LiTaO_3$ or LT) family and potassium titanyl phosphate ($KtiPO_4$ or KTP) and its isomorphs. Typical values of the nonlinear coefficient are of the order 10^{-11} m/V, and the field required to reverse the domains is of the order kV/mm.

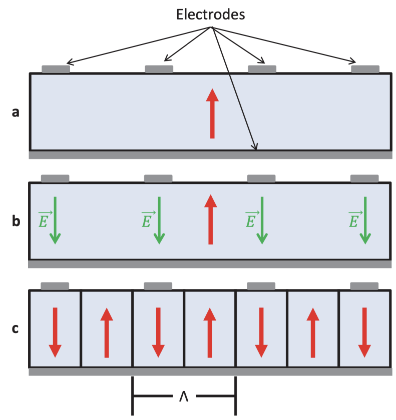

Figure 4: Sketch of the periodic poling method. **a**: All the domains point in the same direction as indicated by the red arrow. **b**: An electric field is applied in the opposite direction causing the inversion of the domains in the affected regions. **c**: We get the desired periodic material [7].

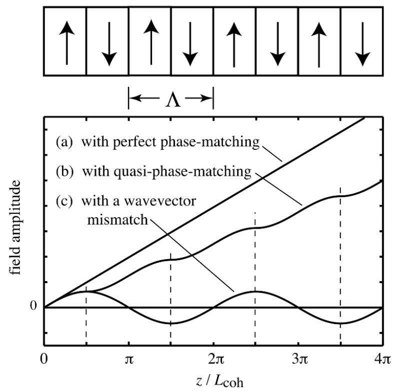

Figure 5: Comparison of the spatial variation of the field amplitude of the generated wave in a nonlinear optical interaction for three different phase matching conditions. L_{coh} is the coherent buildup length, where the poling period Λ is twice the L_{coh} [14].

With periodic poling one can eliminate angle tuning. But because periodic poling is not precise enough to achieve the exact period needed for phase matching, temperature tuning is needed [7]. The refractive index of light n varies with wavelength, temperature, and angle, meaning that temperature dependence of the birefringence of a crystal can help achieve phase matching. It also helps to achieve a precise grating period Λ of the crystal by changing the optical path by using thermal expansion [12, 14].

In order to obtain a measurable SPDC process, the QPM condition must be satisfied, which means equality in Eq. 12 must be true. Considering the angle, we can express the QPM conditions as:

$$k_s \cos\theta_s + k_i \cos\theta_i = k_p - K_G \tag{13}$$

$$k_s \sin\theta_s = k_i \sin\theta_i \, , \tag{14}$$

where θ_s and θ_i are the angles of $\vec{k_s}$ and $\vec{k_i}$ with respect to the pump wave vector $\vec{k_p}$. In the case of

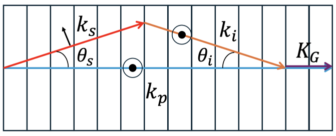

Figure 6: Geometries for SPDC in $x - z$ plane for type-II SPDC in periodically poled nonlinear crystal.

type-II QPM, as shown in Fig. 6, the pump and idler are polarized along the y-axis, and the signal is polarized in the $x - z$ plane.

For collinear type-II SPDC, the refractive indices are given by:

$$n_s(\theta_s, T, \lambda_s) = \frac{n_x(T,\lambda_s)\, n_z(T,\lambda_s)}{\sqrt{n_x^2(T,\lambda_s)\cos^2\theta_s + n_z^2(T,\lambda_s)\sin^2\theta_s}}, \qquad (15)$$
$$n_p = n_y(T,\lambda_p), \quad n_i = n_y(T,\lambda_i)$$

where n_s is the refractive index of the signal as a function of angle θ_s, crystal temperature, and wavelength of the signal λ_s. This is due to the fact that the extraordinary refractive index is dependent on the angle θ from the optical axis and is therefore given by the ellipsoid equation for the indices. When θ_s is small, that is, we are in near-collinear condition, n_s is approximately n_z. Other refractive indices are given by the Sellmeier equation [15], which is an empirical relationship between the refractive index and the wavelength of a particular transparent medium [9]. Since wave vectors in Eq. 12 can be expressed as: $\vec{k_j} = \frac{2\pi \vec{n_j}}{\lambda_j}$, where the subscripts $j = p,\ s,\ i$ denote the pump, signal, and, idler, these refractive indices (Eq. 15) determine k_j's in Eqs. 13 and 14.

For an arbitrary pump wavelength, and desired signal and idler wavelengths, one can calculate the poling period and temperature of the crystal that we need for our desired SPDC process [9, 11].

5 Generation of Polarization Entangled Photon Pairs

There are different methods to generate photon pairs entangled in polarization. Historically, the first methods included a single emitter for type-II SPDC and a sandwich scheme for type-I SPDC. Both methods used birefringent phase matching. For degenerate and collinear SPDC interferometric methods were proposed, which allowed longer crystals and more photons to be collected. For the Mach-Zehnder interferometer, two downconverters were placed in each arm of the interferometer. The disadvantage of this setup is that it requires the interferometer to be phase-stable, and thus usually requires sophisticated stabilization. To avoid this problem, one can use the Sagnac interferometer, which is phase-stable since it uses only one downconverter in a loop-like structure [7].

5.1 Sagnac Interferometer

The Sagnac source of polarized entangled photons is illustrated in Fig. 7. It is generally composed of two mirrors and a polarizing beam splitter (PBS) in a loop-like structure. The advantage is that different polarizations from the PBS travel in different directions along the same path but still travel the same distance. This is where phase stabilization comes from, since changing one path also changes the other. The crystal (PPLN - periodically poled lithium niobate) is placed between two mirrors, meaning that the input beam goes through the crystal twice. This reduces the need for temporal compensation. The crystal is kept at a constant temperature appropriate for degenerate type-II downconversion. The temperature is controlled to $\pm 0.01°$C. Due to the QPM (Eq. 12) it only downconverts horizontally polarized pump ($|H_p\rangle \rightarrow |H_s\rangle, |V_i\rangle$, where subscripts p, s and i represent the pump, signal and idler photons). This helps with imperfections in PBS; since it reflects some of the $|H\rangle$ polarized beam, the QPM condition will ensure that the wrongly reflected beam will not be downconverted.

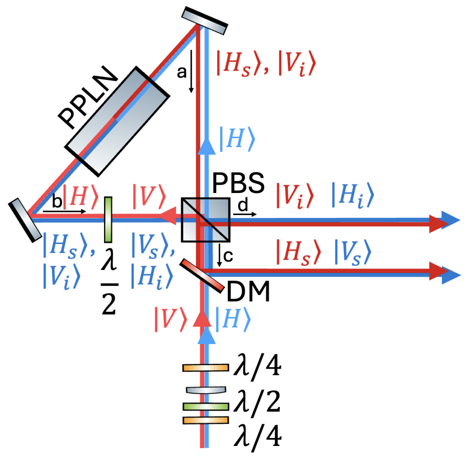

Figure 7: Illustration of the Sagnac interferometer that is a source of entangled photons. Path of horizontal polarization $|H\rangle$ is shown in blue line and path of vertical polarization $|V\rangle$ is shown in red line. The letters a, b, c and d indicate the spatial modes corresponding to all four ports of PBS. To produce the entangled state, one need to use a coherent superposition of the two paths.

The pump polarization is set using a half-wave plate $\left(\frac{\lambda}{2}\right)$ and a quarter-wave plate $\left(\frac{\lambda}{4}\right)$. Another quarter-wave plate is added for finer tuning. The pump polarization state must be a coherent superposition of the polarizations $|H\rangle$ and $|V\rangle$, which means that our incoming pump must be diagonally polarized. Consequently, photon pairs are equally likely to be generated in either clockwise or counter-clockwise emission mode.

There are some additional components in the setup. A plano-convex lens that focuses the beam in the middle of the crystal and improves the signal. A dichroic mirror (DM) that has a cut-off wavelength, where light below this threshold gets transmitted, and light above the threshold gets reflected. This is useful for the separation of pump photons from single photons. Before light goes into a collimator there is also a band-pass filter and a multiplexer, which only allow photons in a certain wavelength interval to pass. This ensures that the counts we obtain are from downconverted photons only.

To get entangled state we first need to split the pump beam by the PBS. The horizontal component of the pump $|H\rangle$ is transmitted by PBS and in the crystal produces pairs $|H_s\rangle_b$, $|V_i\rangle_b$. The half-wave plate within the loop flips $|H_s\rangle_b$, $|V_i\rangle_b$ into $|V_s\rangle_b$, $|H_i\rangle_b$, and after PBS we have $|V_s\rangle_c$, $|H_i\rangle_d$. The vertical component of the pump $|V\rangle$ is reflected by PBS and then rotated by the half-wave plate into $|H\rangle$. In the crystal, it produces pairs $|H_s\rangle_a$, $|V_i\rangle_a$, which are split by PBS, so that we get $|H_s\rangle_c$, $|V_i\rangle_d$. After each loop, the photons interfere in PBS and we get a maximally entangled Bell state:

$$|\psi\rangle = |H_s\rangle_c |V_i\rangle_d + \beta e^{i\phi} |V_s\rangle_c |H_i\rangle_d \tag{16}$$

where β is set using a half-wave plate and is the power ratio between the two clockwise and counterclockwise pumps, and ϕ is controlled by a quarter-wave plate. If we detect a photon with polarization $|H_s\rangle_c$, then we know that the other photon will have polarization $|V_i\rangle_d$. The same holds for the other term [2, 6–8].

6 Entanglement Measurement and Its Interpretation

For characterization of entangled photon pairs, one needs to perform a quantum state tomography and reconstruct the density matrix. One observes photon counts for each channel and coincidences for pairs of channels. Coincidences are events where two photon clicks are recorded at the same time or within a very small time window. Random events are a source of noise in a measurement, which comes from the statistical nature of light.

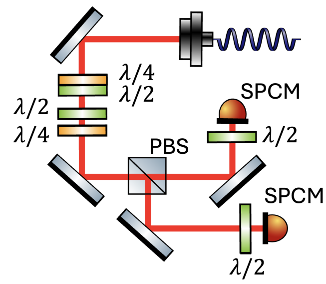

Figure 8: Illustration of the analysis stage where we perform measurements. The beam comes from Sagnac source through single mode fiber and goes into single photon counting modules (SPCM). Path of the beam is indicated by the red line.

To characterize the source, we need an external setup, illustrated in Fig. 8, to make separable projective measurements on each of the photons. The single photons are coupled from the Sagnac source by single-mode fibers and back out into free space. They first pass through the quarter-wave and half-wave plates, which compensate for the drift of polarization of photons in fibers. With the second half-wave and quarter-wave plates one can choose an arbitrary measurement basis.

Since the Sagnac source has two outputs, our analysis stage needs two set-ups that are illustrated in Fig. 8. The setups must be as close to the same as possible to avoid the difference in the optical paths and consequently having delays in photon detection [6, 7].

6.1 Quantum State Tomography

Quantum tomography is the process of reconstructing the density matrix from measurements taken in different projections. The density matrix is reconstructed using the maximum likelihood method, which is explained in detail in Ref. [16].

To perform a measurement, one needs to project the polarization of downconverted beams into different bases from which the density matrix can be reconstructed. Measurements are made in linear, diagonal, and circular bases. The diagonal basis is achieved by rotating the second half-wave plate in Fig. 8 for 22.5° and the circular basis is achieved by rotating the second quarter-wave plate in Fig. 8 for 45° [17]. For each combination for bases, the detectors measure the single counts for each channel and the number of coincidences between pairs of channels. With that, one can reconstruct the density matrix for the state and calculate the characteristic of the entangled state.

6.2 Tomography Results

The reconstructed density matrix can be written as Eq. 3 where non-diagonal matrix components are complex numbers and diagonal matrix components are real numbers. Another way to display the reconstructed density matrix is as a histogram for real and imaginary amplitudes. For an ideal $|\psi^-\rangle$, which we can obtain with type-II SPDC, every element of the density matrix should be 0, except for elements $(|HV\rangle + \langle VH|)\,(|VH\rangle + \langle HV|)$ in the real part, which would be either 0.5 or -0.5. With type-II SPDC, it is also possible to obtain $|\psi^+\rangle$ by changing the phase in Eq. 16, which can be done by rotating the quarter-wave plate for 90°. The density matrix would look different, in particular, elements $(|HV\rangle + \langle VH|)\,(|VH\rangle + \langle HV|)$ in the real part would be positive [6, 7].

The results shown in Figs. 9 and 10 were obtained in the Laboratory for Quantum Entanglement at IJS in Ljubljana. We used a 780 nm laser for pump, a PPLN (periodically poled lithium niobate) crystal with dimensions $50 \times 2 \times 1$ mm for downconversion of collinear and degenerate 1550 nm photons and a 250 mm plano-convex lens. Fidelity with $|\psi^-\rangle$ was $(97.1 \pm 0.08)\,\%$, purity was $(97.9 \pm 0.09)\,\%$ and tangle was $(92.5 \pm 0.07)\,\%$. All characteristic were computed using equations from 3.1.

The results obtained show high tangle and fidelity with the desired state, whereas high purity tells us that the state is not very mixed. The source therefore produces entangled states of high quality and is comparable to others in the literature with a similar layout, such as in Ref. [7]. Compared to other sources of entanglement, such as quantum dots (QD), see Ref. [18], SPDC sources produce photon pairs with low emission probability, while QD are more efficient at producing entangled photon pairs. One pair of entangled photons can be produced on demand with an almost 100 % probability, but they fail short due to their poor quality of the entanglement compared to SPDC sources.

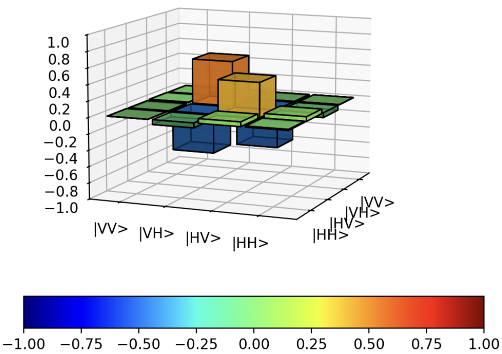

Figure 9: Reconstructed density matrix displayed as a histogram for real amplitudes.

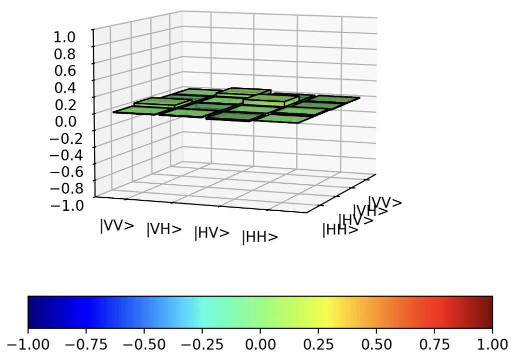

Figure 10: Reconstructed density matrix displayed as a histogram for imaginary amplitudes.

7 Implementation of Experiment Over Record Long Distance

For many quantum applications, mostly the quantum key distribution (QKD), a key technique is a reliable long-distance distribution of entanglement. Physicists from the Austrian Academy of Science have succeeded in entangling photons over 248 kilometers in optical fiber, which is more than double the previous record of 100 kilometers.

The source of entangled photon pairs was stationed in Vienna, where they used SPDC in a Sagnac configuration with a 775.06 nm pump laser. That created downconverted photon pairs in PPLN crystal around 1550.12 nm with $>$ 99% fidelity. One output was sent to Bratislava in Slovakia with a distance of 119 km, and the other was sent to St. Pölten in Austria with a distance of 129 km.

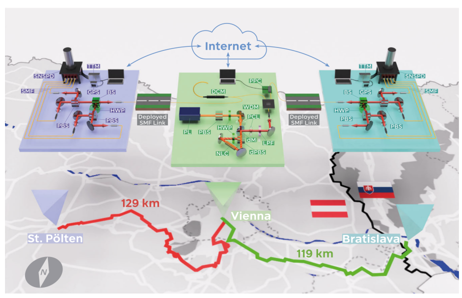

Figure 11: Sketch of the setup for continuous entanglement distribution over a transnational 248 km fiber link [5].

This paves the way for low-maintenance, ultra-stable quantum communication over a long distance that is independent of weather conditions and time of day. This is a significant step towards quantum internet [5].

8 Conclusion

Entanglement has always been an important topic in quantum physics, but has now also become important for quantum technology. It is a basis for the realization of quantum communication that offers fast and secure information transfer over long distances. It is also a very important component of the quantum key distribution and a basis for quantum teleportation. Entanglement is a phenomenon that connects two particles to each other, so that they become inseparable. This allows us to use one of the particles and its measurement to transfer information about the other particle, which remains with us.

Experimentally, in 2022 Neumann et al. [5] managed to reach a distance of 248 km for the entanglement distribution in the deployed fiber. Fiber-based systems offer stable operations, independence from meteorological conditions, and substantially reduced maintenance effort. Compared to satellite connections, these advantages can compensate for their higher losses. Although intercontinental quantum connections will most likely be operated using satellites, shorter distances can be covered by fiber links.

Photons are a great platform for complex quantum experiments, which could represent an important step towards many different practical quantum implementations. In the seminar, I presented a robust and easy method for generating polarization entangled photon pairs. It is a basis for many different quantum applications, the most mature of them being quantum key distribution. It harnesses quantum correlations of entangled photons to produce cryptographic keys of provably unbreakable security. But all of this is just the beginning of the second quantum revolution.

References

[1] P. Schindler, D. Nigg, T. Monz, J. T. Barreiro, E. Martinez, S. X. Wang, S. Quint, M. F. Brandl, V. Nebendahl, C. F. Roos, M. Chwalla, M. Hennrich and R. Blatt, New Journal of Physics **15**, 123012 (2013).

[2] M. Hajdušek and R. V. Meter, *Quantum communications*, 2023.

[3] J. I. Cirac, P. Zoller, H. J. Kimble and H. Mabuchi, Phys. Rev. Lett. **78**, 3221 (1997).

[4] T. E. Northup and R. Blatt, Nature Photonics **8**, 356 (2014).

[5] S. P. Neumann, A. Buchner, L. Bulla, M. Bohmann and R. Ursin, Nature Communications **13**, `10.1038/s41467-022-33919-0` (2022).

[6] A. Goyal, 'Generation and characterization of polarization entangled photon pairs', Master's thesis (The University of Chicago, Chicago, USA, 2022).

[7] D. R. Hamel, 'Realization of novel entangled photon sources using periodically poled materials', Master's thesis (University of Waterloo, Waterloo, Ontario, Canada, 2010).

[8] F. Steinlechner, M. Gilaberte Basset, M. Jofre, T. Scheidl, J. Torres, V. Pruneri and R. Ursin, Journal of the Optical Society of America B **31**, 2068 (2014).

[9] H. J. Lee, H. Kim, M. Cha and H. S. Moon, Applied Physics B **108**, `10.1007/s00340-012-5088-4` (2012).

[10] L. de Forges de Parny, O. Alibart, J. Debaud, S. Gressani, A. Lagarrigue, A. Martin, A. Metrat, M. Schiavon, T. Troisi, E. Diamanti, P. Gélard, E. Kerstel, S. Tanzilli and M. Van Den Bossche, Communications Physics **6**, `10.1038/s42005-022-01123-7` (2023).

[11] C. Couteau, Contemporary Physics **59**, 291 (2018).

[12] D. S. Hum and M. M. Fejer, Comptes Rendus Physique **8**, 180 (2007).

[13] J. A. Armstrong, N. Bloembergen, J. Ducuing and P. S. Pershan, Phys. Rev. **127**, 1918 (1962).

[14] R. W. Boyd, *Nonlinear optics*, 4rd (Academic Press, Inc., USA, 2020).

[15] J. W. Gooch, 'Sellmeier equation', in *Encyclopedic dictionary of polymers*, edited by J. W. Gooch (Springer New York, New York, NY, 2011), pp. 653–654.

[16] R. Blume-Kohout, Physical Review Letters **105**, `10.1103/physrevlett.105.200504` (2010).

[17] I. Drevenšek Olenik and M. Vilfan, *Optika*, Vol. 6 (Fakulteta za matematiko in fiziko, 2023).

[18] Y. Chen, M. Zopf, R. Keil, F. Ding and O. Schmidt, Nature Communications **9**, `10.1038/s41467-018-05456-2` (2018).